

ACO based speed control of SRM fed by photovoltaic system



A.S. Oshaba^a, E.S. Ali^b, S.M. Abd Elazim^{b,*}

^a Research Institute, Power Electronics and Energy Conversions, NRC Bldg., El-Tahrir St., Dokki, 12311 Giza, Egypt

^b Electric Power and Machine Department, Faculty of Engineering, Zagazig University, Zagazig 44519, Egypt

ARTICLE INFO

Article history:

Received 28 November 2013

Received in revised form 26 November 2014

Accepted 1 December 2014

Available online 26 December 2014

Keywords:

Ant colony optimization

Genetic algorithm

High speed SRM

Speed control

PI controller

Photovoltaic system

ABSTRACT

This paper proposes a speed control of Switched Reluctance Motor (SRM) supplied by Photovoltaic (PV) system. The proposed design of the speed controller is formulated as an optimization problem. Ant Colony Optimization (ACO) algorithm is employed to search for the optimal Proportional Integral (PI) parameters of the proposed controller by minimizing the time domain objective function. The behavior of the proposed ACO has been estimated with the behavior of Genetic Algorithm (GA) in order to prove the superior efficiency of the proposed ACO in tuning PI controller over GA. Also, the behavior of the proposed controller has been estimated with respect to the change of load torque, variable reference speed, ambient temperature, and radiation. Simulation results confirm the better behavior of the optimized PI controller based on ACO compared with optimized PI controller based on GA over a wide range of operating conditions.

© 2014 Elsevier Ltd. All rights reserved.

Introduction

Over the past decades, the Switched Reluctance Motors (SRMs) have been the focus of several researches [1,2]. The SRM has a simple, rugged, and low-cost structure. It has no Permanent Magnet (PM) or winding on the rotor. This structure not only reduces the cost of the SRM but also offers high speed operation capability for this motor. Unlike the induction and PM machines, the SRM is capable of high speed operation without the concern of mechanical failures that result from the high level centrifugal force. In addition, the inverter of the SRM drive has a reliable topology. The stator windings are connected in series with the upper and lower switches of the inverter. This topology can prevent the shoot through fault that exists in the induction and permanent motor drive inverter [3,4].

Many techniques have been illustrated to deal with the speed control of SRM. Fuzzy Logic Control (FLC) [5–10], Artificial Neural Network (ANN) [11,12], robust controller [13], and adaptive controller [14] have been employed to solve the problem of speed control of SRM. Moreover, optimization techniques like Genetic Algorithm (GA) [15], Particle Swarm Optimization (PSO) [16–18], Bacteria Foraging [19–23] and BAT algorithm [24] have attracted the attention in designing controller and speed control of various motors.

A new evolutionary algorithm known as Ant Colony Optimization (ACO) algorithm is proposed in this paper to design a robust

speed control of SRM. ACO is multi-agent system in which the behavior of each single agent, called artificial ant is inspired by the behavior of real ants [25]. ACO has been successfully employed to optimization problems in power system such as power quality enhancement [26], optimal reactive power dispatch [27]. The feature of this technique is different from other method since it can be implemented easily and flexible for many problems. Finally its capability in avoiding the occurrences of local optima for a given problem is achieved [28].

ACO is developed in this paper for controlling the speed of SRM supplied by Photovoltaic (PV) system. ACO is used for tuning the PI controller parameters to control the duty cycle of DC/DC converter and therefore speed control of SRM. The design problem of the proposed controller is formulated as an optimization problem and ACO is employed to search for the optimal controller parameters. By minimizing the time domain objective function representing the error between reference speed and actual one, the system performance is improved. Simulation results assure the effectiveness of the proposed controller in providing good speed tracking system over a wide range of load torque, ambient temperature and radiation with minimum overshoot/undershoot and minimal settling time. Also, the results assure the superiority of the proposed ACO method in tuning controller compared with GA.

System under study

The system under study consists of PV system acts as a voltage source for a connected SRM. The speed control loop is designed using ACO. The speed error signal is obtained by comparing the

* Corresponding author. Tel.: +20 1200331213, +20 55 2369750.

E-mail addresses: oshaba68@hotmail.com (A.S. Oshaba), ehabsalimalisalama@yahoo.com (E.S. Ali), sahareldEEP@yahoo.com (S.M. Abd Elazim).

Nomenclature

N_r and N_s	number of rotor and stator poles respectively	V_B and I_B	the output converter voltage and current respectively
q	number of phases	J_t	the objective function
C_r	the commutation ratio	K_p and K_i	the parameters of PI controller
β_s and β_r	the stator and rotor pole arc respectively	n	number of nodes
I and V	module output current and voltage	m	number of ants
I_c and V_c	cell output current and voltage	t_{\max}	maximum iteration
I_{ph} and V_{ph}	the light generation current and voltage	d_{\max}	maximum distance for each ant's tour
I_s	cell reverse saturation current	β	the relative importance of pheromone versus distance ($\beta > 0$)
I_{sc}	the short circuit current	ρ	heuristically defined coefficient ($0 < \rho < 1$)
I_o	the reverse saturation current	α	pheromone decay parameter ($0 < \alpha < 1$)
R_s	the module series resistance	q_a	parameter of the algorithm ($0 < q_a < 1$)
T	cell temperature	τ_o	initial pheromone level
K	Boltzmann's constant	d_i	distance between two nodes
q_o	electronic charge	u	unvisited node
KT	(0.0017 A/°C) short circuit current temperature coefficient	r	current node
G	solar illumination in W/m ²	τ_{ij}	the pheromone trail deposited between node i and j by ant k
E_g	band gap energy for silicon	η_{ij}	the visibility and it equals to the inverse of the distance ($\eta_{ij} = 1/d_{ij}$)
A	ideality factor	T^k	the path effectuated by the ant k at a given time
T_r	reference temperature		
I_{or}	cell rating saturation current at T_r		
n_s	series connected solar cells		
k_i	cell temperature coefficient		
k	the duty cycle of the Pulse Width Modulation (PWM)		

reference speed and the actual one. The output of the ACO controller is denoted as duty cycle. The schematic block diagram is shown in Fig. 1.

Construction of SRM

The construction of a 8/6 (8 stator poles, 6 rotor poles) poles SRM has doubly salient construction [14]. The windings of the SRM are simpler than those of other types of motors, and winding exists only on stator poles, and is simply wound on it with no winding on the rotor poles. The winding of opposite poles is connected in series or in parallel forming a number of phases, and exactly half the number of stator poles, and the excitation of a single phase excites two stator poles. The rotor has a simple laminated salient pole structure without winding. SRMs have the advantage of reducing copper losses while its rotor is winding. Its stampings are made preferably of silicon steel, especially in higher efficiency applications [29,30]. The construction of an 8/6 SRM is shown in Fig. 2.

Torque is developed in SRMs due to the tendency of the magnetic circuit to adopt the configuration of minimum reluctance.

The magnetic behavior of the SRM is highly nonlinear. The static torque produced by one phase at any rotor position is calculated using the following equations [30,31].

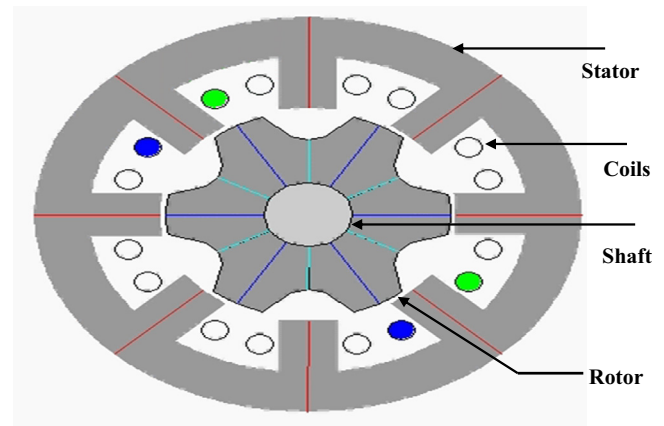


Fig. 2. The SRM 8/6 poles construction.

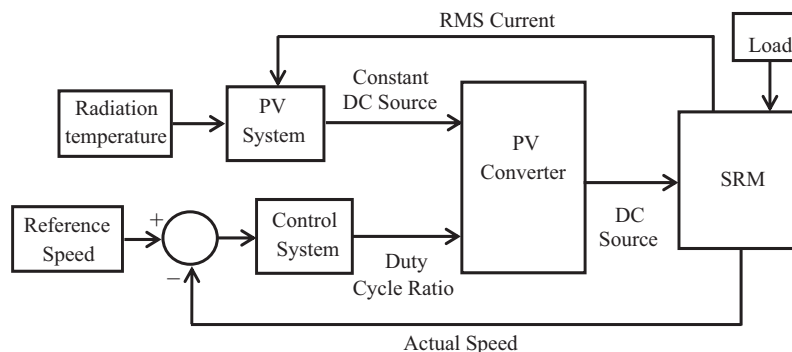


Fig. 1. The overall system for SRM control.

$$\text{Co energy} = W' = \int \psi(\theta, i) di \quad (1)$$

$$\text{Static torque} = T_{static} = dW'/d\theta \quad (2)$$

From Eqs. (1) and (2) a similar static torque matrix can be estimated where current will give the row index and θ will give the column index as in [30,31]. The value of developed torque can be calculated from the static torque look up table by using second order interpolation method between the current value and θ .

The value of actual speed can be calculated from the following mechanical equations:

$$d\omega/dt = (T(\theta, i) - T_{mech})/J \quad (3)$$

where the speed error is the difference between the rotor and reference speed. The value of rotor angular displacement θ can be calculated from the following equation:

$$d\theta/dt = \omega \quad (4)$$

The angle δ corresponding to the displacement of phase A in relation to another phase is given by:

$$\delta = 2\pi \left(\frac{1}{N_r} - \frac{1}{N_s} \right) \quad (5)$$

The positive period of phase is determined by the following equation:

$$\text{duty period} = 2\pi \left(\frac{1}{qN_r} \right) C_r \quad (6)$$

C_r can be calculated by the following equation.

$$C_r = 2\pi \left(\frac{1}{\beta_r} - \frac{1}{\beta_s} \right) \quad (7)$$

Duration of negative current pulses is depended on the stored energy in phase winding. On running, the algorithm is corrected by PI controller. This method is suitably with special range for turn on angle. The parameters of SRM are shown in appendix.

Photovoltaic system

Mathematical modeling of solar cell is an important step in the analysis and design of PV control systems. The PV mathematical model can be obtained by applying the fundamental physical laws governing the nature of the components making the system [32].

To overcome the variations of illumination, temperature, and load resistance, voltage controller is required to track the new modified reference voltage whenever load resistance, illumination and temperature variation occurs. I - V characteristics of solar cell are given by the following equations [33,34]:

$$I_c = I_{ph} - I_o \left\{ e^{\left[\frac{q_0}{AKT} (V_c + I_c R_s) \right]} - 1 \right\} \quad (8)$$

$$V_c = \frac{AKT}{q_0} \ln \left(\frac{I_{ph} + I_o - I_c}{I_o} \right) - I_c R_s \quad (9)$$

$$I = I_{ph} - I_o \left\{ e^{\left[\frac{q_0}{n_s AKT} (V + n_s I R_s) \right]} - 1 \right\} \quad (10)$$

$$V = \frac{n_s AKT}{q_0} \ln \left(\frac{I_{ph} + I_o - I}{I_o} \right) - n_s I R_s \quad (11)$$

where

$$I_{ph} = \frac{G}{1000} [I_{sc} + k_i (T - T_r)] \quad (12)$$

$$I_o = I_{or} \left(\frac{T}{T_r} \right)^3 e^{\left[\frac{q_0 E_g}{AK} \left(\frac{1}{T_r} - \frac{1}{T} \right) \right]} \quad (13)$$

The module output power can be determined simply from

$$P = V \cdot I \quad (14)$$

PV system is used in this paper to power SRM. The parameters of PV system are given in appendix.

DC-DC converter

Many converters have been used and tested; buck converter is a step down converter, while boost converter is a step up converter [35,36]. In this paper, a hybrid (buck and boost) DC/DC converter is used. The equations for this converter type in continuous conduction mode are:

$$V_B = \frac{-k}{1-k} V_{ph} \quad (15)$$

$$I_B = \frac{k-1}{k} I_{ph} \quad (16)$$

where k is the duty cycle of the Pulse Width Modulation (PWM) switching signal. V_B and I_B are the output converter voltage and current respectively. The Matlab/Simulink of PV system can be simulated as shown in Fig. 3.

Objective function

A performance index can be defined by the Integral of Time multiply Absolute Error (ITAE). Accordingly, the objective function J_t is set to be:

$$J_t = \int_0^{\infty} t(|e|) dt \quad (17)$$

where $e = w_{reference} - w_{actual}$.

Based on this J_t optimization problem can be stated as: minimize J_t subjected to:

$$K_p^{\min} \leq K_p \leq K_p^{\max}, \quad K_i^{\min} \leq K_i \leq K_i^{\max} \quad (18)$$

Ranges of PI controllers are [0.001–20]. This paper focuses on optimal tuning of PI controller for speed tracking of SRM using ACO algorithm. The aim of the optimization process is to search for the optimum controller parameters setting that minimize the difference between reference speed and actual one.

Overview of ant colony optimization algorithm

The first ACO algorithm was introduced by Marco Dorigo [25]. The development of this algorithm was inspired by the observation of ant colonies. The behavior that provided the inspiration for ACO is the ants' foraging behavior, and in particular, how ants can find shortest paths between food sources and their nest. When searching for food, ants initially explore the area surrounding their nest in a random manner. While moving, ants leave a chemical pheromone trail on the ground. The pheromone quantity depends on the length of the path and the quality of the discovered food source [37]. An ant chooses an exact path in connection with the intensity of the pheromone. The pheromone trail evaporates over time if no more pheromone is laid down. Other ants are attracted to follow the pheromone trail. Therefore, the path will be marked again and it will attract more ants to use the same path. The pheromone trail on paths leading to rich food sources close to the nest will be more frequented and will therefore grow faster. In this way, the best solution has more intensive pheromone and higher probability to be chosen. The described behavior of real ant colonies can be

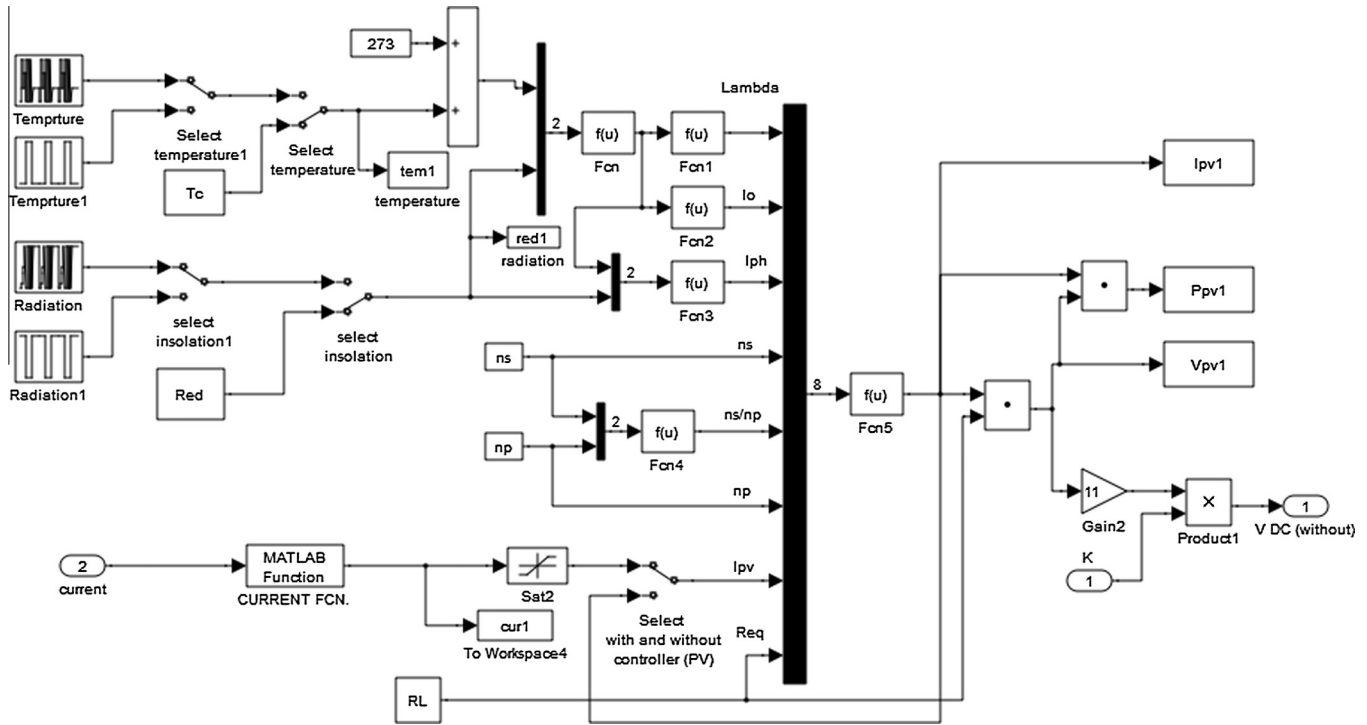


Fig. 3. Matlab/Simulink for PV system.

used to solve optimization problems in which artificial ants search the solution space by transiting from nodes to nodes. The artificial ants movement usually associated with their previous action that stored in the memory with a specific data structure [38]. The pheromone consistencies of all paths are updated only after the ant finished its tour from the first node to the last node. Every artificial ant has a constant amount of pheromone stored in it when the ant proceeds from the first node. The pheromone that has been stored will be evenly distributed on the path after artificial ants finished its tour. The amount of pheromone will be high if artificial ants finished its tour with a good path and vice versa. The pheromone of the routes progressively decreases by evaporation in order to avoid artificial ants stuck in local optima solution [37,38]. The ACO algorithm can be divided into the following steps:

Step 1: initialization

In this step, the following parameters (n , m , t_{\max} , d_{\max} , β , ρ , α , q_a , and τ_o) of ACO algorithm are initialized.

The maximum distance for every ant's tour d_{\max} can be calculated using the following equation:

$$d_{\max} = \max \left[\sum_{i=1}^{n-1} d_i \right] \quad (19)$$

$$d_i = |r - \max(u)| \quad (20)$$

Step 2: provide first position

Generate first position randomly; the first node will be selected by generating a random number according to a uniform distribution, ranging from 1 to n .

Step 3: transition rule

The probability for an ant k at node i to choose next node j can be expressed as:

$$P_{ij}^k(t) = \frac{[\tau_{ij}(t)]^\alpha [\eta_{ij}(t)]^\beta}{\sum_{ij \in T^k} [\tau_{ij}(t)]^\alpha [\eta_{ij}(t)]^\beta}; \quad i, j \in T^k \quad (21)$$

Step 4: local pheromone updating

Local updating pheromone is different from ant to other because each ant takes a different route. The initial pheromone of each ant is locally updated as shown below.

$$\tau_{ij}(t+1) = (1 - \rho)\tau_{ij}(t) + \rho\tau_o \quad (22)$$

Step 5: fitness function

After all ants attractive to the shortest path that having a strongest pheromone, the best solution of the objective function is obtained.

Step 6: global pheromone updating

Amount of pheromone on the best tour becomes the strongest due to attractive of ants for this path. Moreover, the pheromone on the other paths is evaporated in time. The pheromone level is updated by applying the following equation:

$$\tau_{ij}(t+1) = (1 - \alpha)\tau_{ij}(t) + \alpha\Delta\tau_{ij}(t) \quad (23)$$

Step 7: program termination

The program will be terminated when the maximum iteration is reached or the best solution is obtained without the ants stagnations. The proposed procedure steps are shown in Fig. 4. The parameters of ACO are shown in appendix.

Results and simulations

In this section, the superiority of the proposed ACO algorithm over GA [39,40] in designing PI controller for speed control of SRM is illustrated. Fig. 5 shows the variations of objective function with two optimization techniques. The objective functions decrease monotonically over generations of ACO and GA. Moreover, ACO converges at a faster rate (35 generations) compared with GA (50 generations). Also, computational time (CPU) of both algorithms is compared based on the average CPU time taken to converge the solution. The average CPU for ACO is 32.1 s while it is 43.9 s for GA. The mentioned CPU time is the average of 10

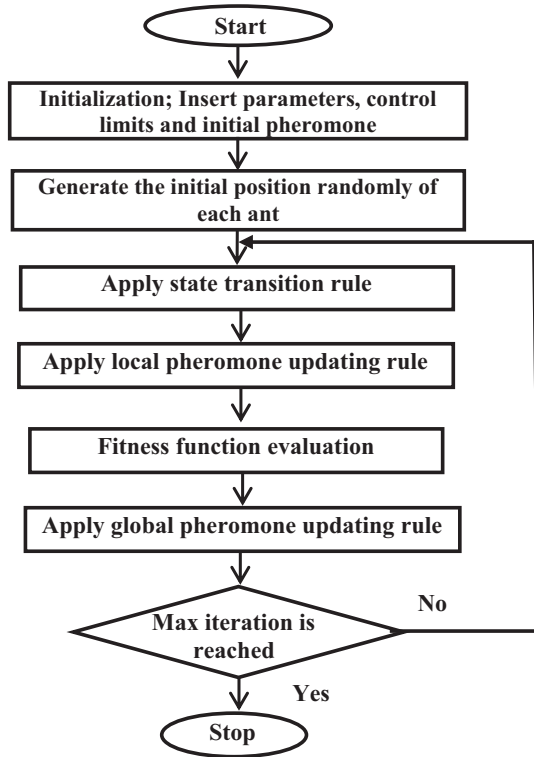


Fig. 4. Flow chart of the proposed ACO algorithm.

executions of the computer code. The proposed ACO and GA are programmed using MATLAB 7.1 with Intel(R) Core(TM) I5 and 4.00 GB of RAM. Table 1 shows the parameters of PI controller, average settling time, and average percentage overshoot based on two optimization techniques. It can be seen that the time domain characteristics for ACO are smaller than GA. Hence, compared with GA, ACO greatly improves the time domain characteristics of SRM.

Response under step change in load torque

Fig. 6, shows the step change in load torque of SRM. The speed response and control signal for this case are shown in Figs. 7 and 8 respectively. These figures indicate the capability of the ACO in

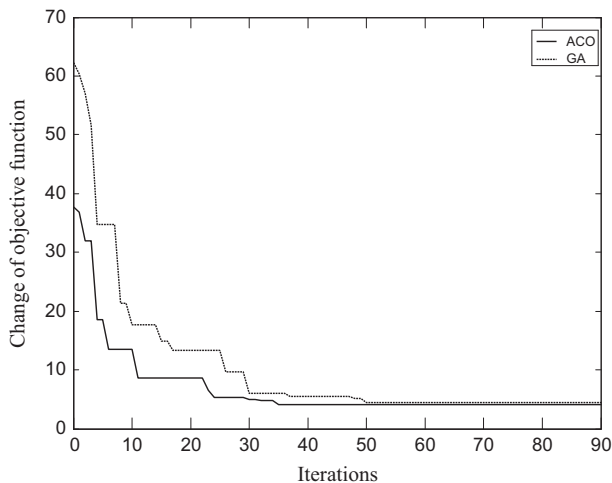


Fig. 5. Change of objective function for different optimization techniques.

Table 1 Comparison between ACO and GA.

	K_p	K_i	Average settling time (s)	Average percentage over shoot
ACO	0.0349	8.0125	0.057	16.13
GA	0.0126	8.6354	0.063	17.02

reducing the settling time and system oscillations over GA. Moreover, the actual speed tracks the reference speed rapidly. The settling time is approximately 0.06, and 0.064 s for ACO and GA respectively. Hence, the proposed ACO is capable of providing sufficient speed tracking compared with GA.

Response under variable reference speed and load torque

In this case, the system responses under variation of reference speed and load torque are obtained. Fig. 9 shows the variation of the load torque as an input disturbance while the parameters of PV system are constant. Moreover, the system responses for different controllers are shown in Figs. 10 and 11. It is clear from these figures, that the proposed ACO algorithm outperforms and outlasts GA in controlling the speed of SRM and reducing settling time effectively. Therefore, compared with GA based controller, ACO based controller greatly enhances the system performance.

Response under variable load torque, reference speed and PV parameters

In this case, variations of load torque, reference speed and PV parameters are applied. Fig. 12 shows the change of load torque, radiation and temperature respectively. Moreover, the system responses for both controllers are shown in Figs. 13 and 14. It is clear from these figures, that the proposed ACO is more efficient in improving speed control of SRM compared with GA. Also, the proposed controller has a smaller settling time and system response is quickly driven with the reference speed. Thus, the potential and superiority of the proposed ACO over GA is demonstrated.

Robustness and performance indices

To demonstrate the robustness of the proposed controller, three different performance indices are used. These indices are: The Integral Absolute value of the Error (IAE), the Integral of the Square

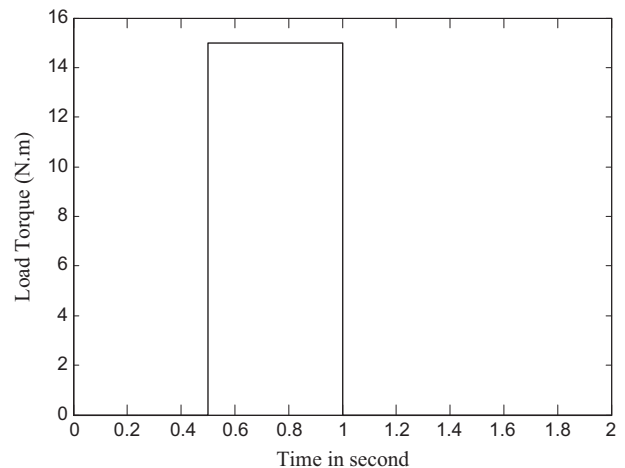


Fig. 6. Step change in load torque.

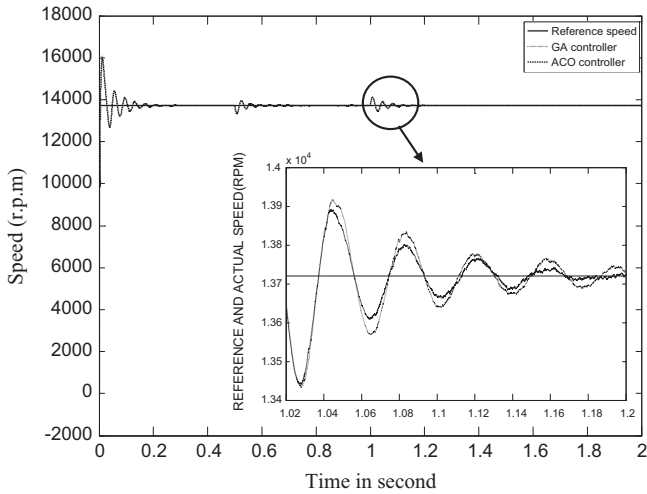


Fig. 7. Change in speed due to step load torque.

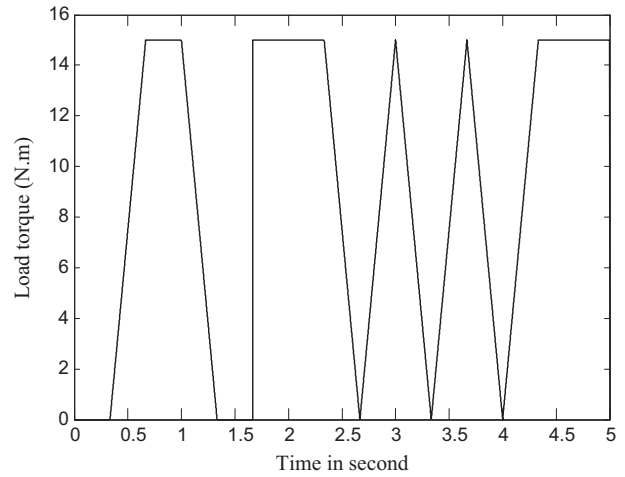


Fig. 9. Change in load torque.

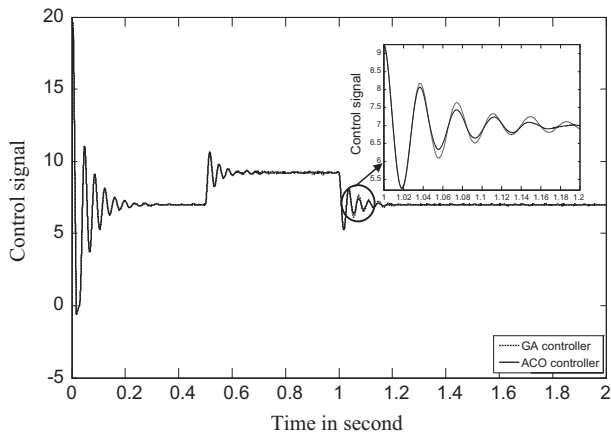


Fig. 8. Change in control signal due to step load torque.

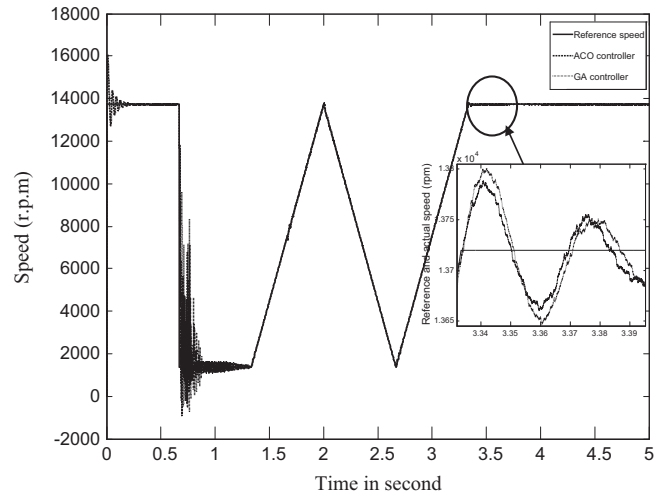


Fig. 10. Change in speed for variable load torque and reference speed.

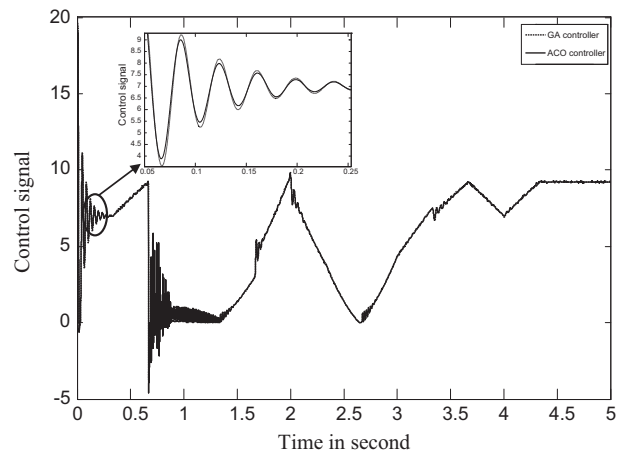


Fig. 11. Change in control signal for variable load torque and reference speed.

value of the Error (ISE), and the Integral of the Time multiplied Square value of the Error (ITSE). It is worth mentioning that the smaller the value of these indices, the better the system response in terms of time domain characteristics. Numerical results of performance robustness for variations of load torque, reference speed, and PV parameters are listed in Table 2. It can be seen that the values of these indices corresponding to ACO are smaller compared with those of GA. This demonstrates that the overshoot, undershoot and settling time are reduced by applying the proposed ACO based controller.

Conclusions

In this paper, a novel method for speed control of SRM (8/6 poles) is proposed via ACO. The design problem of the proposed controllers is formulated as an optimization problem and ACO is employed to search for optimal parameters of PI controller. By minimizing the time domain objective function in which the difference between the reference and actual speed are involved; speed control of SRM is improved. Simulation results emphasis that the designed ACO based PI controller is robust in its operation and gives a superb performance for the change in load torque, reference speed, radiation and temperature over GA based PI controller. Besides the simple architecture of the proposed controller, it has the potentiality of implementation in real time environment.

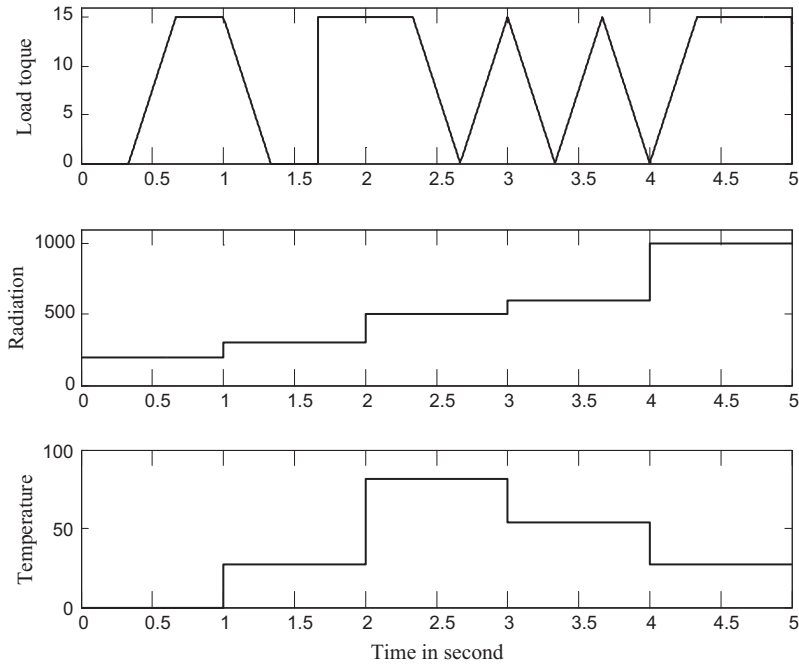


Fig. 12. Change in load torque, radiation and temperature.

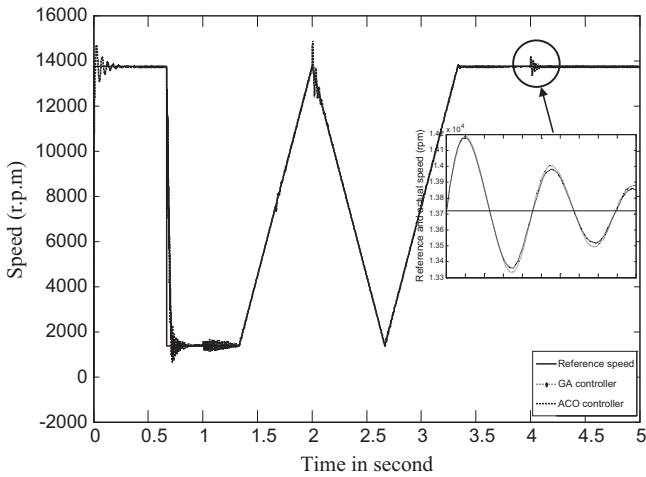


Fig. 13. Change in speed for different controllers.

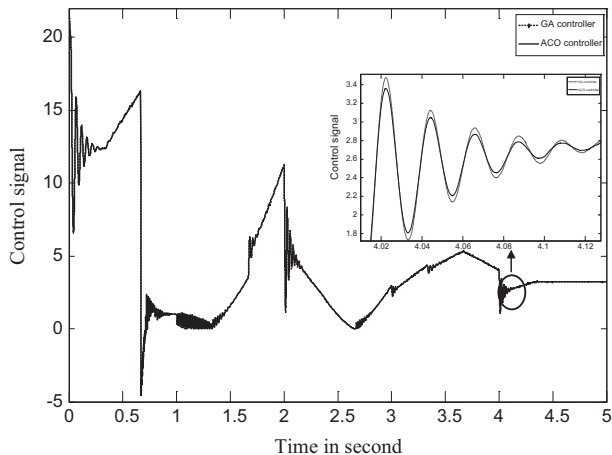


Fig. 14. Change in control signal for different controllers.

Table 2

Values of performance indices.

	Performance index		
	IAE	ISE	ITSE
ACO	12.0937	19.1421	72.1439
GA	13.3529	20.9312	76.3588

Appendix

The parameters of the studied system are as shown below:

- (a) SRM parameters: $N_s = 8$, $N_r = 6$, rating speed = 13,700 r.p.m, $C_r = 0.8$, $q = 4$, phase resistance of stator = 17 ohm, phase inductance of aligned position = 0.605 H, phase inductance of unaligned position = 0.1555 H, step angle = 15°.
- (b) PV parameters: $A = 1.2153$; $E_g = 1.11$; $I_{or} = 2.35e-8$; $I_{sc} = 4.8$; $T_r = 300$; $K = 1.38e-23$; $n_s = 36$; $q_o = 1.6e-19$; $k_i = 0.0021$.
- (c) Genetic parameters: max generation = 100; population size = 50; crossover probabilities = 0.75; mutation probabilities = 0.1.
- (d) ACO parameters: $n = 10$, $m = 5$, $t_{max} = 5$, $d_{max} = 49$, $\beta = 2$, $\rho = 0.6$, $\alpha = 0.1$, $q_a = 0.6$, $\tau_o = 0.1$.

References

- [1] Miller TJE. Switched reluctance motors and their control. London: Oxford Science Publications; 1993.
- [2] Veltman A, Pulle DWJ, Doncker RD. Fundamentals of electrical drives. Springer-Verlag; 2007 [ISBN: 978-1-4020-5503-4].
- [3] Gieras JF. Advancements in electric machines. Springer; 2009 [ISBN: 978-1-4020-9006-6].
- [4] Doncker RD, Pulle DWJ, Veltman A. Advanced electrical drives: analysis, modeling, control. Springer; 2011 [ISBN 978-94-007-0181-6].
- [5] Chen H, Zhang D, Cong ZY, Zhang ZF. Fuzzy logic control for switched reluctance motor drive. In: Proceedings of the first int conf on machine learning and cybernetics, Beijing, 4–5 November; 2002. p. 145–9.
- [6] Jie X, Changliang X. Fuzzy logic based adaptive PID control of switched reluctance motor drive. In: Proceedings of the 26th Chinese control conf, July 26–31; 2007, Zhangjiajie, Hunan, China. p. 41–5.

- [7] Karakas E, Vardarbasi S. Speed control of SR motor by self-tuning fuzzy PI controller with artificial neural network. *Sadhana* 2007;32(5):587–96.
- [8] Gupta RA, Bishnoi SK. Sensorless control of switched reluctance motor drive with fuzzy logic based rotor position estimation. *Int J Comput Appl* 2010;1(22):72–9.
- [9] Hashem GM, Hasanien HM. Speed control of switched reluctance motor based on fuzzy logic controller. In: Proceedings of the 14th international middle east power systems conf (MEPCON'10), Cairo University, Egypt, December 19–21; 2010. p. 288–92.
- [10] Rares T, Virgil C, Lorand S, Calin M. Artificial intelligence based electronic control of switched reluctance motors. *J Comput Sci Control Syst* 2011;4(1):193–8.
- [11] Xia CL, Xiu J. RBF ANN nonlinear prediction model based adaptive PID control of switched reluctance motor drive. In: 13th Int conf, ICONIP 2006, Hong Kong, China, October 3–6; 2006, Proceedings Part III. p. 626–35.
- [12] Ali BS, Hasanien HM, Galal Y. Speed control of switched reluctance motor using artificial neural network controller. *Comput Int Inf Technol Commun Comput Inf Sci* 2011;250:6–14.
- [13] Rajendran A, Padma S. H-infinity robust control technique for controlling the speed of switched reluctance motor. *Front Electr Electron Eng* 2012;7(3):337–46.
- [14] Yousef AM. Switched reluctance motor sensorless fed by photovoltaic system based on adaptive PI controller. *Eng Res J (ERJ)* 2012;35(4):333–42 [Minoufiya University].
- [15] Elmas C, Yigit T. Genetic algorithm based on-line tuning of a PI controller for a switched reluctance motor drive. *Electr Power Compon Syst* 2007;35:675–91.
- [16] Mahendiran TV, Thanushkodi K, Thangam P. Speed control of switched reluctance motor using new hybrid particle swarm optimization. *J. Comput Sci* 2012;8(9):1473–7.
- [17] Oshaba AS, Ali ES. Speed control of induction motor fed from wind turbine via particle swarm optimization based pi controller. *Res J Appl Sci, Eng Technol* 2013;5(18):4594–606.
- [18] Oshaba AS, Ali ES. Swarming speed control for DC permanent magnet motor drive via pulse width modulation technique and DC/DC converter. *Res J Appl Sci, Eng Technol* 2013;5(18):4576–83.
- [19] Oshaba AS, Ali ES. Bacteria foraging: a new technique for speed control of DC series motor supplied by photovoltaic system. *Int J WSEAS Trans Power Syst* 2014:185–95.
- [20] Abd-Elazim SM, Ali ES. Synergy of particle swarm optimization and bacterial foraging for TCSC damping controller design. *Int J WSEAS Trans Power Sys* 2013;8(2):74–84.
- [21] Ali ES, Abd-Elazim SM. Power system stability enhancement via bacteria foraging optimization algorithm. *Int Arab J Sci Eng (AJSE)* 2013;38(3):599–611.
- [22] Ali ES, Abd-Elazim SM. Coordinated design of PSSs and SVC via bacteria foraging optimization algorithm in a multimachine power system. *Int J Electr Power Energy Syst* 2012;41(1):44–53.
- [23] Abd-Elazim SM, Ali ES. Bacteria foraging optimization algorithm based SVC damping controller design for power system stability enhancement. *Int J Electr Power Energy Syst* 2012;43(1):933–40.
- [24] Ali ES. Optimization of power system stabilizers using BAT search algorithm. *Int J Electr Power Energy Syst* 2014;61(C):683–90.
- [25] Colorni A, Dorigo M, Maniezzo V. Distributed optimization by ant colonies. In: Proceedings of the first European conf on artificial life. Elsevier Science Publisher; 1992. p. 134–42.
- [26] Chitra N, Prabaakaran K, Senthil Kumar A, Munda J. Ant colony optimization adopting control strategies for power quality enhancement in autonomous microgrid. *Int J Comput Appl* 2013;63(13):34–8.
- [27] Abou El-Ela AA, Kinawy AM, Mouwafi MT, El Sehiemy RA. Optimal reactive power dispatch using ant colony optimization algorithm. In: Proceedings of the 14th int middle east power systems conf (MEPCON'10), Cairo University, Egypt, December 19–21; 2010. p. 960–5.
- [28] Blum C. Ant colony optimization: introduction and recent trends. *Phys Life Rev* 2005;2:353–73.
- [29] Vijayakumar K, Karthikeyan R, Paramasivam S, Arumugam R, Srinivas KN. Switched reluctance motor modeling, design, simulation, and analysis: a comprehensive review. *IEEE Trans Magn* 2008;44(12):4605–17.
- [30] Oshaba AS. Performance of a sensorless SRM drive fed from a photovoltaic system. *Res J Appl Sci, Eng Technol* 2013;6(17):3165–73.
- [31] Oshaba AS. Control strategy for a high speed SRM fed from a photovoltaic source. *Res J Appl Sci, Eng Technol* 2013;6(17):3174–80.
- [32] Saied MM, Hanafy AA. A contribution to the simulation and design optimization of photovoltaic systems. *IEEE Trans. Energy Convers.* 1991;6:401–6.
- [33] Hussein K, Muta I, Hoshino T, Oskada M. Maximum photovoltaic power tracking; an algorithm for rapidly changing atmospheric conditions. *IEEE Proc Gener, Transm Distrib* 1995;142(1):59–64.
- [34] Lu CF, Liu CC, Wu CJ. Dynamic modeling of battery energy storage system and application to power system stability. *IEE Proc Gener, Transm Distrib* 1995;142(4):429–35.
- [35] Bose BK. *Modern power electronics and AC drives*. New Jersey: Prentice-Hall; 2002.
- [36] Lin PZ, Hsu CF, Lee TT. Type-2 fuzzy logic controller design for buck DC–DC converters. In: Proceedings of the IEEE int conf on fuzzy systems; 2005. p. 365–70.
- [37] Kalil MR, Musirin I, Othman MM. Ant colony based optimization technique for voltage stability control. In: Proceedings of the 6th WSEAS int conf on power systems, Lisbon, Portugal, September 22–24; 2006. p. 149–54.
- [38] Omar M, Soliman M, Abdel Ghany AM, Bendary F. Ant colony optimization based PID for single area load frequency control. *Int J Electr Power Eng* 2013;7(3):65–70.
- [39] Chambers LD. *The practical handbook of genetic algorithms: applications*. 2nd ed. Chapman and Hall/CRC; 2000.
- [40] Simon D. *Evolutionary optimization algorithms*. 1st ed. Wiley; 2013.